1

2

3

4 **ORIGINAL ARTICLE:**

5 Effective sequestration of *Clostridium difficile* protein toxins by calcium aluminosilicate

6

7

8

9 **RUNNING TITLE:** *Clostridium difficile* toxin sequestration

10

11

12

13

14 Joseph M. Sturino[a,#], Karina Pokusaeva[a] and Robert Carpenter[b,c]

15

16

17 [a] Nutrition and Food Science Department, Texas A&M University,

18 College Station, Texas 77843

19 [b] Texas EnteroSorbents, Inc., Bastrop, Texas 78602

20 [c] Salient Pharmaceuticals Incorporated, Houston, Texas 77005

21

22

23

24

25 [#] **Corresponding Author:** Dr. Joseph M. Sturino;

26 Telephone: +1 (805) 317-4243; E-Mail: joseph.sturino@gmail.com;

27 URL: www.josephsturino.com/

28
29

30
31

32   **ABSTRACT:**

33   *Clostridium difficile* is a leading cause of antibiotic-associated diarrhea and the

34   etiologic agent responsible for *C. difficile* infection. TcdA and TcdB are nearly

35   indispensible virulence factors for *Clostridium difficile* pathogenesis. Given the toxin-

36   centric mechanism by which *C. difficile* pathogenesis occurs, the selective sequestration

37   and neutralization of TcdA and TcdB by non-antibiotic agents represents a novel mode of

38   action to prevent or treat *C. difficile*-associated disease. In this preclinical study, we used

39   quantitative enzyme immunoassays to determine the extent by which a novel drug,

40   calcium aluminosilicate uniform particle size Novasil (CAS UPSN M-1), is capable of

41   sequestering TcdA and TcdB *in vitro*. The following major findings were derived from

42   the present study: Firstly, CAS UPSN M-1 efficiently sequestered both TcdA and TcdB

43   to undetectable levels. Secondly, we show that CAS UPSN M-1's affinity for TcdA is

44   greater than its affinity for TcdB. Lastly, we show that CAS UPSN M-1 exhibited limited

45   binding affinity for non-target therapeutic proteins. Together, these results suggest that

46   ingestion of calcium aluminosilicate might protect gastrointestinal tissues from antibiotic-

47   or chemotherapy-induced *C. difficile* infection by neutralizing the cytotoxic and pro-

48   inflammatory effects of luminal TcdA and TcdB.

49

50

51   **KEYWORDS:** *Clostridium difficile*, TcdA, TcdB, calcium aluminosilicate,

52   gastrointestinal inflammation, quantitative enzyme immunoassay

53

INTRODUCTION

54

55   *Clostridium difficile* is a leading cause of antibiotic-associated diarrhea (AAD)

56   and the etiologic agent responsible for *C. difficile*-associated infection (CDI). CDI

57   typically starts as a mild diarrhea but rapidly degenerates into a variety of potentially life-

58   threatening conditions, including sepsis syndrome and pseudomembranous colitis (1). In

59   the United States, approximately 330,000 cases of CDI are estimated each year (2);

60   however the incidence of *C. difficile* infection continues to increase (2-3). Increasing CDI

61   rates highlight that current infection control procedures and treatment options are

62   insufficient.

63   In the healthcare setting, endospore-forming *C. difficile* are transmitted to patients

64   via the fecal-oral route (4). Following exposure, the host's gastrointestinal microbiota

65   typically either quells a nascent *C. difficile* infection or suppresses it to sub-clinical levels

66   (5). As a result of the latter, approximately 20% of hospitalized adults become

67   asymptomatic *C. difficile* carriers, while carriage rates approach 50% for patients in long-

68   term care (6-9). The likelihood of developing CDI increases in patients with dysbiotic

69   gastrointestinal microbiota, since *C. difficile* can thrive in the dysbiotic niche (5, 10). This

70   dysbiosis is often the result of non-specific chemotherapies that are used to treat

71   conditions unrelated to *C. difficile* infection (*e.g*., antibacterial agents or antineoplastic

72   drugs).

73   The antibiotics metronidazole and vancomycin are currently used to treat CDI

74   (11). Unfortunately, given the conflicting roles of antibiotics in the establishment and

75   resolution of CDI, *C. difficile* AAD is recurrent in up to 1 in 5 patients (12). These

76   already high reoccurrence rates are expected to increase if *C. difficile* strains with

77   intermediate- and complete-resistance to metronidazole and vancomycin emerge (13).

78   Together, these alarming trends illustrate an urgent need to develop novel and efficacious

79   therapeutics to treat CDI, including non-traditional therapeutic agents.

80   *C. difficile* is an extracellular pathogen and it typically does not invade host

81   tissues. While a number of *C. difficile*-encoded virulence factors are responsible for *C.*

82   *difficile* carriage and pathogenesis, toxin A (TcdA) and toxin B (TcdB) are among the

83   best-studied (14). Once secreted into the colon, these cytotoxic protein-based enzymes

84   are translocated across the membrane bilayer and into the cytosol by receptor-mediated

85   endocytosis (15). Once inside the cell, these glycosyltransferases trigger altered cellular

86   transcription, which results in significant cellular apoptosis and tissue remodeling (16-

87   18). TcdA and TcdB are also strongly pro-inflammatory, which exacerbates their effects

88   on structural and functional changes in tissue integrity (19-20). Together, these

89   inflammation-related activities contribute to the progressive ablation of gastrointestinal

90   function that is characteristic of CDI. In animal models, the administration of purified *C.*

91   *difficile* TcdA induces the hallmark symptoms of an acute, pseudomembranous colitis-

92   like condition: edema, gastrointestinal inflammation, cellular necrosis, and gastroenteritis

93   in the absence of the bacterium (19, 21-23). The administration of TcdB elicits similar

94   effects, albeit to a lesser degree (22, 24). As a result, these protein-based enzymes have

95   been ascribed as nearly indispensible determinants for *C. difficile* pathogenesis.

96   Given the toxin-centric mechanism by which *C. difficile* pathogenesis occurs, the

97   selective sequestration and neutralization of TcdA and TcdB by non-antibiotic agents

98   represents a novel mode of action to prevent or treat *C. difficile*-associated diseases (25-

99   26). To date, four *C. difficile* toxin-binding agents have been examined in pre-clinical

100   studies: cholestyramine, colestipol, synsorb 90, and tolevamer (25). Of these toxin-

101   binding agents, only three have been tested in clinical studies. Unfortunately, none of

102   these agents have proven to be as efficacious as traditional antibiotic therapies.

103   Nevertheless, it is important to continue to develop new candidate therapies. In this

104   manuscript, we describe the characterization of CAS UPSN M-1, a novel calcium

105   aluminosilicate agent that has been developed to selectively bind to and neutralize large

106   clostridial protein toxins. Calcium aluminosilicate is recognized by the Food and Drug

107   Administration (FDA) as a Generally Regarded as Safe (GRAS) additive, which can be

108   supplemented to foods at levels up to 2% (w/w) (27).

109
110   **MATERIALS AND METHODS**
111
112   **Protein-based cytotoxic enzymes and reagents.** Lyophilized *C. difficile* TcdA

113   and *C. difficile* TcdB were stored according to the manufacturer's specification

114   (Calbiochem, Gibbstown, NJ). TcdA and TcdB were resuspended in 10 mM 2,2-

115   bis(hydroxymethyl)-2,2′,2-nitrilotriethanol (Bis-Tris) buffer (Sigma-Aldrich, St. Louis,

116   MO) and maintained on ice prior to being assayed. All other chemicals were molecular

117   biology grade and stored as recommended by the manufacturer. A SevenMulti

118   conductivity meter (Mettler Toledo, Columbus, OH) was used for pH measurements.

119   **Putative toxin binding agent.** Calcium aluminosilicate uniform particle size

120   Novasil M-1 (CAS UPSN M-1), the novel sequestering agent used in this study, was

121   provided by Salient Pharmaceuticals Incorporated (Houston, TX).

122   **Quantitative enzyme immunoassay (qEIA) for toxin quantification.** The

123   concentration of *C. difficile* TcdA or TcdB was measured using the Premier Toxins A&B

124 enzyme immunoassay (EIA) according to the manufacture's instructions (Meridian

125 Bioscience Inc., Cincinnati, OH) except that a series of assay positive control samples

126 (*i.e.*, TcdA and TcdB reference standards at a range of known concentrations) was

127 incorporated into each repeated measurement; the concentration of these reference

128 standards typically ranged from 5 to 20 ng/ml. In brief, the resultant qEIA uses *C.*

129 *difficile* TcdA- and TcdB-specific polyclonal antibodies to capture TcdA and TcdB and to

130 non-covalently anchor them to the solid-phase EIA support matrix. Matrix-bound toxins

131 were subsequently complexed with horseradish peroxidase (HRP)-conjugated mouse

132 anti-toxin A (monoclonal) or goat anti-toxin B (polyclonal) antibodies, respectively.

133 After the removal of unbound HRP-antibody conjugates, degradation of urea hydrogen

134 peroxide by toxin-bound horseradish peroxidase was assayed in the presence of the

135 reducing co-substrate 3,3′,5,5′-tetramethyl-[1,1′-biphenyl]-4,4′-diamine (TMB).

136 Phosphoric acid (1 M) was used to arrest the reaction. The terminal chromophore

137 benzidine-4,4′-diimine (BZDI), an oxidized derivative of TMB, was measured in

138 arbitrary units (AU) at an optical density of 450 nm ($OD_{450\ nm}$) using an Infinite M200

139 microplate reader (Tecan US Inc., Durham, NC). The Infinite M200 iControl software

140 was used to generate custom EIA microplate templates to speed data acquisition and to

141 ensure accurate sample assignation.

142   **Toxin sequestration assays.** This qEIA was used to assess the sequestration (an

143 aggregate of adsorption and absorption) of large clostridial protein toxins by calcium

144 aluminosilicate. Unless otherwise indicated, calcium aluminosilicate was suspended up to

145 a final concentration of 0.5 mg/ml in 10 mM Bis-Tris (pH 6.5) and pre-equilibrated to

146 37°C in a Thermomixer R shaking incubator (Eppendorf, Hauppauge, NY) equipped with

147   a 1.5-ml block with constant agitation at 1,200 revolutions per minute (rpm). Individual

148   sequestration reactions were started by the addition of the toxin to a final concentration of

149   10 ng/ml (TcdA) or 15 ng/ml (TcdB), unless otherwise indicated. Sequestration reactions

150   were then incubated for 10 min at 37°C with constant agitation at 1,200 rpm in a

151   Thermomixer R (Eppendorf). The sequestration reaction was stopped when the residual

152   calcium aluminosilicate and calcium aluminosilicate-bound toxin complexes were

153   pelleted by centrifugation (2 min at $21,130 \times g$) in a 5424 bench top centrifuge

154   (Eppendorf). Following centrifugation, the clarified supernatant was carefully removed

155   by aspiration, transferred to a 1.5 ml tube, and chilled on ice prior to toxin quantification

156   using the qEIA described above.

157   **Heterologous, non-therapeutic protein-binding and SDS-PAGE.** Calcium

158   aluminosilicate (5 mg/ml) was co-incubated with the SeeBlue Plus2 protein ladder (750

159   µg/ml; Invitrogen, San Diego, CA), which contains a number of non-therapeutic target

160   proteins. Samples were incubated at 37°C for 20 min with constant agitation (1,200 rpm).

161   The reaction was stopped when the residual calcium aluminosilicate and calcium

162   aluminosilicate-bound protein complexes were pelleted by centrifugation (2 min at

163     $21,130 \times g$) in an Eppendorf 5424 bench top centrifuge (Eppendorf). The supernatant

164   was carefully transferred to a fresh tube and set on ice. The pellet containing the residual

165   calcium aluminosilicate and calcium aluminosilicate-bound protein complexes was re-

166   suspended in 1 volume buffer and agitated for 20 min at (1,200 rpm). The unbound

167   calcium aluminosilicate and calcium aluminosilicate-bound protein complexes were

168   again pelleted by centrifugation (2 min at $21,130 \times g$). The resultant pellet eluate—

169   including any proteins eluted from the calcium aluminosilicate—was carefully transferred

170 to a fresh tube. Negative control samples (*i.e.*, SeeBlue Plus2 devoid of calcium

171 aluminosilicate) were otherwise treated identically to experimental samples.

172   The original supernatant and the pellet eluate were both subjected to

173 polyacrylamide gel electrophoresis (PAGE). Samples (15 µl) were loaded into the 1-mm

174 wells of a NuPAGE Novex Tris-Acetate gel (Invitrogen) using 1× lithium dodecyl sulfate

175 (LDS) sample buffer (Invitrogen). Protein electrophoresis was carried out (150 V for 1 h)

176 in an Xcell SureLock Mini Cell (Invitrogen) and 1× NuPAGE tris-acetate SDS running

177 buffer (Invitrogen). Proteins were stained using the SimplyBlue Safe Stain (Invitrogen)

178 according to the manufacturer's instruction. The results were captured using the

179 FluorChem HD2 documentation system with a 5 MHz cooled digital CCD camera (Alpha

180 Innotech).

181   **Biostatistics.** Raw qEIA data were captured using the Infinite M200 i-Control

182 software, exported to Excel (Microsoft Corporation, Redmond, WA), and analyzed using

183 Prism (GraphPad Software Inc., La Jolla, CA). Unless otherwise indicated, data

184 represent at least three repeated measures. Data are expressed as the mean ($\bar{x}$) ± either the

185 standard error of the mean (SEM) or standard deviation (SD), as noted. Calibration

186 curves were generated by least-squares regression. ANOVA was used to determine the

187 statistical significance of the measured differences between treatments. When significant

188 differences were detected by ANOVA, Bonferroni tests were performed *posthoc* in order

189 explore these differences. An associated *p* value of less than 0.05 was considered

190 statistically significant. The base-10 logarithm (log_{10}) of each data point was calculated

191 and a calibration curve for the interpolation of unknowns was generated using least-squares

192 linear regression.

193
194 **RESULTS**

195   **Optimization of a quantitative enzyme immunoassay (qEIA) to detect TcdA**

196 **and TcdB.** Samples containing known concentrations of TcdA or TcdB were used to

197 generate standard curves. The standard curves from each of six randomly selected vials of

198 TcdB are plotted in **FIGURE 1.** A one-factor ANOVA found toxin vial-specific effects

199 were statistically significant ($p < 0.0051$); however, *posthoc* comparisons using the

200 Bonferroni test indicated that—with the exception of one obvious outlier ($p < 0.05$)—

201 differences between the remaining five curves were statistically nonsignificant ($p > 0.05$).

202 For this experimental subset ($n = 5$), the Pearson product-moment correlation coefficient

203 (r) indicated a strong, co-linear relationship between toxin concentration and optical

204 density that was statistically significant between inter-experimental EIA replicates ($r =$

205 0.9078, $p = 0.0047$). Similar results were seen for TcdA ($n = 5$), although differences

206 between individual vials of TcdA were statistically nonsignificant ($p = 0.8707$). As seen

207 with TcdB, a strong co-linear relationship between toxin concentration and optical

208 density was observed. This co-linear relationship was statistically significant between

209 inter-experimental qEIA replicates ($r = 0.9973$, $p = 0.0027$). In separate experiments that

210 examined the effect of toxin thermostability, differences in qEIA reactivity following

211 short-term (*e.g.*, 8 h) incubation on ice were found to be statistically nonsignificant ($p >$

212 0.05). As a result, individual toxin vials were used to conduct multiple sequestration

213 assays within a single workday and were then discarded.

214   **Data distribution and transformation.** The descriptive statistic skewness (g_1)

215 and the Kolmogorov-Smirnov (K-S) normality test were used to examine the data

216 distribution within the TcdA and TcdB datasets. While both datasets skewed right

217   (TcdA: g_1 = 0.6626; TcdB: g_1 = 1.331), the K-S test indicated that neither exhibited

218   significant differences from the Gaussian distribution ($p > 0.10$). Nevertheless, the base-

219   10 logarithm (log_{10}) of each datapoint was calculated to normalize the data. Linear

220   regressions of mean TcdA (n = 4; R^2 = 0.968) and TcdB (n = 5; R^2 = 0.966) reference

221   curves are plotted in **FIGURE 2.** Signal response plateaus were observed at very high

222   toxin concentrations and very low toxin concentrations (data not shown).

223   **Calcium aluminosilicate does not affect the pH of the qEIA.** In order to

224   determine if calcium aluminosilicate might artificially diminish the sensitivity of the

225   qEIA by affecting the pH of the buffer system, calcium aluminosilicate was

226   supplemented to a final working concentration of 0.5 mg/ml in 100 mM Tris (pH 6.5) and

227   the pH was measured (n = 3) once the mixture was equilibrated to 37°C. Incorporation of

228   calcium aluminosilicate up to 0.5 mg/ml did not affect the pH of the buffer system ($\bar{x}$ =

229   6.52, SD = 0.01) when compared to a buffer control that was devoid of calcium

230   aluminosilicate ($\bar{x}$ = 6.50, SD = 0.001), as expected.

231   **Effective, dose-dependent sequestration of large *C. difficile* cytotoxic enzymes**

232   **by calcium aluminosilicate.** Calcium aluminosilicate was assessed for its ability to

233   reduce the concentration of large clostridial protein-based cytotoxic enzymes *in vitro*.

234   During these dose-response experiments, the concentration of TcdA or TcdB (**FIGURE**

235   **3**) was fixed at 10 ng/ml, while the calcium aluminosilicate concentration was varied

236   100-fold (*i.e.*, 0.05 mg/ml, 0.075 mg/ml, 0.1 mg/ml, 0.3 mg/ml, 0.5 mg/ml, 0.75 mg/ml, 1

237   mg/ml, 2 mg/ml, 3 mg/ml, and 5 mg/ml). Calcium aluminosilicate efficiently sequestered

238   TcdA and TcdB *in vitro*. Differences in mean endpoint $OD_{450\ nm}$ between the assay

239   negative control (*i.e.,* vehicle devoid of TcdA) samples ($\bar{x}$ = 0.044 AU, SD = 0.001 AU)

240   and experimental samples supplemented with calcium aluminosilicate up to 2 mg/ml ($\bar{x} =$

241   0.049 AU, SD = 0.004 AU), 3 mg/ml ($\bar{x} =$ 0.049 AU, SD = 0.005 AU), and 5 mg/ml ($\bar{x} =$

242   0.048 AU, SD = 0.004 AU) were statistically nonsignificant ($p > 0.05$).

243   The raw qEIA measurements obtained from experimental samples were converted

244   to residual toxin concentrations using intra-experimental EIA calibration curves.

245   Differences in residual TcdA concentration between the assay positive control (*i.e.*,

246   TcdA-containing samples devoid of calcium aluminosilicate) samples and experimental

247   samples containing calcium aluminosilicate supplemented up to 0.05 mg/ml ($\bar{x} =$ 11.11

248   ng/ml, SD = 1.82 ng/ml), 0.075 mg/ml ($\bar{x} =$ 11.35 ng/ml, SD = 0.22 ng/ml), and 0.1

249   mg/ml ($\bar{x} =$ 10.93 ng/ml, SD = 0.06 ng/ml) were statistically nonsignificant (**FIGURE 3**).

250   In contrast, statistically significant differences in residual TcdA concentrations were

251   measured between the assay positive control and experimental samples containing

252   calcium aluminosilicate supplemented to 0.3 mg/ml ($\bar{x} =$ 8.54 ng/ml, SD = 1.19 ng/ml, *p*

253   < 0.05), 0.5 mg/ml ($\bar{x} =$ 4.88 ng/ml, SD = 0.80 ng/ml, $p < 0.001$), 0.75 mg/ml ($\bar{x} =$ 3.20

254   ng/ml, SD = 0.65 ng/ml, $p < 0.001$), 1 mg/ml ($\bar{x} =$ 1.67 ng/ml, SD = 0.71 ng/ml), 2 mg/ml

255   ($\bar{x} =$ below the lower limit of detection (bLLD), $p < 0.001$), 3 mg/ml ($\bar{x} =$ bLLD, $p <$

256   0.001), and 5 mg/ml ($\bar{x} =$ bLLD, $p < 0.001$). The lower limit of detection for this qEIA is

257   approximately 1.4 ng/ml for TcdA and 2.4 ng/ml for TcdB.

258   The efficiency by which the calcium aluminosilicate calcium aluminosilicate

259   sequestered TcdB was also explored (**FIGURE 3**). Differences in endpoint $OD_{450\ nm}$

260   measurements between the assay negative control (*i.e.,* vehicle devoid of TcdB) samples

261   ($\bar{x} =$ 0.047 AU, SD = 0.004 AU) and experimental samples supplemented with calcium

262   aluminosilicate up to 3 mg/ml ($\bar{x} =$ 0.043 AU, SD = 0.001 AU), and 5 mg/ml ($\bar{x} =$ 0.041

263 AU, SD = 0.002 AU) were statistically nonsignificant ($p > 0.05$). As performed with

264 TcdA, the raw qEIA measurements were converted to residual toxin concentrations.

265 Differences in residual TcdB concentration between the assay positive control (*i.e.*,

266 TcdB-containing samples devoid of calcium aluminosilicate) samples and experimental

267 samples containing calcium aluminosilicate supplemented up to 0.05 mg/ml ($\bar{x} = 9.07$

268 ng/ml, SD = 0.06 ng/ml), 0.075 mg/ml ($\bar{x} = 8.75$ ng/ml, SD = 0.05 ng/ml), 0.1 mg/ml ($\bar{x} =$

269 9.02 ng/ml, SD = 1.38 ng/ml), and 0.3 mg/ml ($\bar{x} = 8.44$ ng/ml, SD = 0.8 ng/ml) were

270 statistically nonsignificant ($p > 0.05$). In contrast, statistically significant differences in

271 residual TcdB concentrations were measured between the assay positive control and

272 experimental samples containing calcium aluminosilicate supplemented up to 0.5 mg/ml

273 ($\bar{x} = 6.27$ ng/ml, SD = 0.36 ng/ml, $P < 0.001$), 0.75 mg/ml ($\bar{x} = 5.47$ ng/ml, SD = 0.64

274 ng/ml; $p < 0.001$), 1 mg/ml ($\bar{x} = 4.99$ ng/ml, SD = 1.23 ng/ml), 2 mg/ml ($\bar{x} = 3.75$ ng/ml;

275 $p < 0.001$), 3 mg/ml ($\bar{x} =$ bLLD, $p < 0.001$), and 5 mg/ml ($\bar{x} =$ bLLD, $p < 0.001$).

276   **The protein-binding activity of calcium aluminosilicate.** The selectivity of

277 calcium aluminosilicate's protein-binding activity was explored further using a variation

278 of the *C. difficile* toxin-binding assay described above. During these experiments,

279 calcium aluminosilicate (5 mg/ml) was challenged with a commercial protein cocktail

280 that contained a number of non-therapeutic proteins, including myosin, bovine serum

281 albumin, and glutamate dehydrogenase. A representative SDS-PAGE gel of the

282 supernatant and the pellet eluate can be found in **FIGURE 4**. CAS UPSN M-1 bound

283 non-therapeutic proteins, but did so with varying efficiency. Indeed, CAS UPSN M-1

284 bound myosin and bovine serum albumin inefficiently, while glutamate dehydrogenase

285 was bound efficiently. Attempts to elute proteins bound to CAS UPSN M-1 were

286 unsuccessful (**FIGURE 4**, lanes 4-5), which suggests that proteins bound to CAS UPSN

287 M-1 are bound tightly.

288

289 <div align="center">**DISCUSSION**</div>

290   The initial toxin concentrations used in this study were selected because they

291 approximated the median concentration of TcdA (4.3 ng/ml) that is typically found in the

292 stool of patients with *C. difficile*-associated diarrhea (range 0.6 ng/ml to 19 µg/ml) (28).

293 As such, the developed qEIA protocol enabled *C. difficile* TcdA and TcdB quantification

294 at clinically relevant concentrations. No hook effect was obvious for either toxin at toxin

295 concentrations between 5 to 15 ng/ml, which constituted the linear range for this qEIA.

296 The high-dose hook effect occurs when the antigen negatively affects the binding

297 capacity of the reporter antibody or when it is added in excess of the reporter antibody

298 (29). The intra-experimental EIA calibration curves generated using this qEIA protocol

299 enabled toxin quantification via interpolation and, thus, facilitated the conversion of

300 optical density measurements to residual toxin concentrations. Furthermore, given the

301 high degree of reproducibility, this qEIA supported inter-experimental comparisons

302 between repeated measurements (*e.g.*, randomized block experiments).

303   This assay revealed that calcium aluminosilicate efficiently removed both TcdA

304 and TcdB at physiologically relevant concentrations. Indeed, calcium aluminosilicate

305 neutralized TcdA to sub-clinical levels *in vitro*. Like tolevamer, protein binding by

306 calcium aluminosilicate does not occur in a generalized or otherwise indiscriminate

307 fashion and, thus, displays a degree of target specificity. Tolevamer is an anionic, high-

308 molecular-weight polymer (>400 kDa) that was developed to neutralize TcdA and TcdB.

309   Tolevamer has been shown to ameliorate CDI-like symptoms in hamsters (30). In

310   addition, tolevamer has demonstrated therapeutic efficacy in a number of phase II and

311   phase III clinical studies (25-26). While effective, tolevamer's cure rate was found to be

312   inferior to those of vancomycin and metronidazole (26, 31). Surprisingly, however, the

313   rate of CDI reoccurrence was generally lower with tolevamer than with either

314   vancomycin or metronidazole (26)

315   TcdA and TcdB are postulated to be paralogs (32-33). As a result, these proteins

316   share significant amino acid sequence similarity to one another—especially at their

317   amino- and carboxy-terminal regions.   Both toxins share approximately 47% identity to

318   each other and approximately 68% sequence similarity (data not shown).   Both proteins

319   are comprised of three well-characterized functional domains (15). The amino-terminus

320   of the protein encodes a peptidase C80-type glycosyltransferase domain and a proximal

321   substrate recognition domain. The hydrophobic middle region is putatively involved in

322   membrane translocation. The carboxy terminus of the protein encodes the clostridial

323   repetitive oligopeptides (CROPS)—also known as cell wall binding (CWB) domains.

324   The carboxy-terminal CROPS facilitate calcium-dependent host cell recognition (33), and

325   may also play a role in the sequestration of TcdA and TcdB by calcium aluminosilicate.

326   Proteins that are evolutionarily and/or structurally related to TcdA and TcdB might also

327   be viable therapeutic targets for calcium aluminosilicate, however additional research is

328   required to test this hypothesis.

329   In addition to the similarities noted above, a number of toxin-specific differences

330   were also observed. For example, the lowest experimental concentration of calcium

331   aluminosilicate for which there was no observable effect was 0.1 mg/ml for TcdA, but 0.3

332   mg/ml for TcdB. The minimum effective concentration (*i.e.*, the threshold dose) for

333   calcium aluminosilicate was 0.3 mg/ml for TcdA, but 0.5 mg/ml for TcdB. Under these

334   conditions, the calcium aluminosilicate concentration that achieved maximum efficacy

335   (EC_{100}) was 2 mg/ml for TcdA, but the concentration of calcium aluminosilicate that

336   provided approximately 50% of the maximum effect (EC_{50}) for TcdA was 0.5 mg/ml. In

337   contrast the EC_{100} and EC_{50} for TcdB were 3 mg/ml and 1 mg/ml, respectively. While

338   calcium aluminosilicate sequesters both protein-based cytotoxic enzymes, these results

339   suggest that its affinity for TcdA is greater than its affinity for TcdB.

340   As antibiotic resistant pathogens continue to emerge, the development of non-

341   antibiotic treatment options represents a timely therapeutic approach to CDI management.

342   Calcium aluminosilicate exhibited potent *C. difficile* TcdA- and TcdB-neutralizing

343   activity and selective protein binding *in vitro*. Given the well-documented safety profile

344   of calcium aluminosilicate (34), these studies provide *in vitro* evidentiary support our

345   hypothesis that ingestion of calcium aluminosilicate might protect gastrointestinal tissues

346   and accelerate a patient's recovery from antibiotic- or chemotherapy-induced, *C. difficile*-

347   associated diarrhea by neutralizing the cytotoxic effects of luminal TcdA and TcdB.

348   Depending on its relative effectiveness and tolerability during downstream clinical

349   studies, CAS UPSN M-1, the novel sequestration agent described in this study, may be

350   used to complement or, possibly, replace existing antibiotic therapies for the treatment of

351   CDI. However, it is beyond the scope of this current study to examine the biological

352   effects of calcium aluminosilicate *in vivo*.

353

354

372 **REFERENCES**
373
374 1. **Eaton SR, Mazuski JE.** 2013. Overview of severe *Clostridium difficile* infection.
375 Crit. Care Clin. **29:**827-839.
376 2. **Lessa FC, Gould CV, McDonald LC.** 2012. Current status of *Clostridium*
377 *difficile* infection epidemiology. Clin. Infect. Dis. **55**(Suppl 2)**:**S65-70.
378 3. **Gerding DN.** 2010. Global epidemiology of *Clostridium difficile* infection in
379 2010. Infect. Control Hosp. Epidemiol. **31**(Suppl 1)**:**S32-34.
380 4. **Sunenshine RH, McDonald LC.** 2006. *Clostridium difficile*-associated disease:
381 new challenges from an established pathogen. Cleve. Clin. J. Med. **73:**187-197.
382 5. **Britton RA, Young VB.** 2014. Role of the intestinal microbiota in resistance to
383 colonization by *Clostridium difficile*. Gastroenterology. **146:**1547-1553.
384 6. **Riggs MM, Sethi AK, Zabarsky TF, Eckstein EC, Jump RL, Donskey CJ.**
385 2007. Asymptomatic carriers are a potential source for transmission of epidemic
386 and nonepidemic *Clostridium difficile* strains among long-term care facility
387 residents. Clin. Infect. Dis. **45:**992-998.
388 7. **Ryan J, Murphy C, Twomey C, Paul Ross R, Rea MC, MacSharry J, Sheil B,**
389 **Shanahan F.** 2010. Asymptomatic carriage of *Clostridium difficile* in an Irish
390 continuing care institution for the elderly: prevalence and characteristics. Ir. J.
391 Med. Sci. **179:**245-250.
392 8. **Rea MC, O'Sullivan O, Shanahan F, O'Toole PW, Stanton C, Ross RP, Hill**
393 **C.** 2012. *Clostridium difficile* carriage in elderly subjects and associated changes
394 in the intestinal microbiota. J. Clin. Microbiol. **50:**867-875.
395 9. **Hung YP, Lee JC, Lin HJ, Liu HC, Wu YH, Tsai PJ, Ko WC.** 2014. Clinical
396 impact of *Clostridium difficile* colonization. J. Microbiol. Immunol. Infect.
397 10. **Pérez-Cobas AE, Artacho A, Ott SJ, Moya A, Gosalbes MJ, Latorre A.** 2014.
398 Structural and functional changes in the gut microbiota associated to *Clostridium*
399 *difficile* infection. Front. Microbiol. **5:**335.
400 11. **Luciano JA, Zuckerbraun BS.** 2014. *Clostridium difficile* infection:
401 prevention, treatment, and surgical management. Surg. Clin. North Am.
402 **94:**1335-1349.
403 12. **Fekety R, McFarland LV, Surawicz CM, Greenberg RN, Elmer GW,**
404 **Mulligan ME.** 1997. Recurrent *Clostridium difficile* diarrhea: characteristics of
405 and risk factors for patients enrolled in a prospective, randomized, double-blinded
406 trial. Clin. Infect. Dis. **24:**324-333.
407 13. **Shah D, Dang MD, Hasbun R, Koo HL, Jiang ZD, DuPont HL, Garey KW.**
408 2010. *Clostridium difficile* infection: update on emerging antibiotic treatment
409 options and antibiotic resistance. Expert Rev. Anti. Infect. Ther. **8:**555-564.
410 14. **Awad MM, Johanesen PA, Carter GP, Rose E, Lyras D.** 2014. *Clostridium*
411 *difficile* virulence factors: insights into an anaerobic spore-forming pathogen. Gut
412 Microbes. 1:0.
413 15. **Voth DE, Ballard JD.** 2005. *Clostridium difficile* toxins: mechanism of action
414 and role in disease. Clin. Microbiol. Rev.**18:**247-263.
415 16. **Just I, Gerhard R.** 2004. Large clostridial cytotoxins. Rev. Physiol. Biochem.
416 Pharmacol. **152:**23-47.

417   17.   **Feltis BA, Wiesner SM, Kim AS, Erlandsen SL, Lyerly DL, Wilkins TD,**
418   **Wells CL.** 2000. *Clostridium difficile* toxins A and B can alter epithelial
419   permeability and promote bacterial paracellular migration through HT-29
420   enterocytes. Shock. **14:**629-634.

421   18.   **Farrow MA, Chumbler NM, Lapierre LA, Franklin JL, Rutherford SA,**
422   **Goldenring JR, Lacy DB.** 2013. *Clostridium difficile* toxin B-induced necrosis is
423   mediated by the host epithelial cell NADPH oxidase complex. Proc. Natl. Acad.
424   Sci. U.S.A. **110:**18674-18679.

425   19.   **Hirota SA, Iablokov V, Tulk SE, Schenck LP, Becker H, Nguyen J, Al Bashir**
426   **S, Dingle TC, Laing A, Liu J, Li Y, Bolstad J, Mulvey GL, Armstrong GD,**
427   **MacNaughton WK, Muruve DA, MacDonald JA, Beck PL.** 2012. Intrarectal
428   instillation of *Clostridium difficile* toxin A triggers colonic inflammation and
429   tissue damage: development of a novel and efficient mouse model of *Clostridium*
430   *difficile* toxin exposure. Infect. Immun. 80(12):4474-84.

431   20.   **Vohra P, Poxton IR.** 2012. Induction of cytokines in a macrophage cell line by
432   proteins of *Clostridium difficile*. FEMS Immunol Med Microbiol. 65:96-104.

433   21.   **Lyerly DM, Saum KE, MacDonald DK, Wilkins TD.** 1985. Effects of
434   *Clostridium difficile* toxins given intragastrically to animals. Infect. Immun.
435   **47:**349-352.

436   22.   **Lima AA, Lyerly DM, Wilkins TD, Innes DJ, Guerrant RL.** 1988. Effects of
437   *Clostridium difficile* toxins A and B in rabbit small and large intestine *in vivo* and
438   on cultured cells *in vitro*. Infect. Immun. **56:**582-588.

439   23.   **Sun X, Savidge T, Feng H.** 2010. The enterotoxicity of *Clostridium difficile*
440   toxins. Toxins (Basel). **2:**1848-80.

441   24.   **Savidge TC, Pan WH, Newman P, O'brien M, Anton PM, Pothoulakis C.**
442   2003. *Clostridium difficile* toxin B is an inflammatory enterotoxin in human
443   intestine. Gastroenterology.**125:**413-420.

444   25.   **Weiss K.** 2009. Toxin-binding treatment for *Clostridium difficile*: a review
445   including reports of studies with tolevamer. Int. J. Antimicrob. Agents. **33:**4-7.

446   26.   **Bauer MP, van Dissel JT.** 2009. Alternative strategies for *Clostridium difficile*
447   infection. Int. J. Antimicrob. Agents. **33**(Suppl 1)**:**S51-56.

448   27.   **Electronic Code of Federal Regulations**. 2010. 21 CFR §182.2729.

449   28.   **Solomon K, Webb J, Ali N, Robins RA, Mahida YR.** 2005. Monocytes are
450   highly sensitive to *Clostridium difficile* toxin A-induced apoptotic and
451   nonapoptotic cell death. Infect. Immun. **73:**1625-1634.

452   29.   **Fernando SA, Wilson GS.** 1992. Studies of the 'hook' effect in the one-step
453   sandwich immunoassay. J. Immunol. Methods. **151:**47-66.

454   30.   **Barker RH Jr, Dagher R, Davidson DM, Marquis JK.** 2006. Review article:
455   tolevamer, a novel toxin-binding polymer: overview of preclinical pharmacology
456   and physicochemical properties. Aliment. Pharmacol. Ther. **24:**1525-1534.

457   31.   **Louie TJ, Peppe J, Watt CK, Johnson D, Mohammed R, Dow G, Weiss K,**
458   **Simon S, John JF Jr, Garber G, Chasan-Taber S, Davidson DM; Tolevamer**
459   **Study Investigator Group.** 2006. Tolevamer, a novel nonantibiotic polymer,
460   compared with vancomycin in the treatment of mild to moderately severe
461   *Clostridium difficile*-associated diarrhea. Clin. Infect. Dis. **43:**411-420.

462   32.   **Hofmann F, Herrmann A, Habermann E, von Eichel-Streiber C.** 1995.
463   Sequencing and analysis of the gene encoding the alpha-toxin of *Clostridium*
464   *novyi* proves its homology to toxins A and B of *Clostridium difficile*. Mol. Gen.
465   Genet. **247:**670-679.
466   33.   **Demarest SJ, Salbato J, Elia M, Zhong J, Morrow T, Holland T, Kline K,**
467   **Woodnutt G, Kimmel BE, Hansen G.** 2005. Structural characterization of the
468   cell wall binding domains of *Clostridium difficile* toxins A and B; evidence that
469   Ca2+ plays a role in toxin A cell surface association. J. Mol. Biol. **346:**1197-
470   1206.
471   34.   **Mitchell NJ, Kumi J, Aleser M, Elmore SE, Rychlik KA, Zychowski KE,**
472   **Romoser AA, Phillips TD, Ankrah NA.** 2014. Short-term safety and efficacy of
473   calcium montmorillonite clay (UPSN) in children. Am. J. Trop. Med. Hyg.
474   **91:**777-85.
475
476
477
478

479

480

481

482
483
484
485

486
487
488
489
490
491
492
493
494
495
496
497
498
499
500
501
502
503
504
505
506
507
508
509
510
511
512
513
514
515
516
517
518
519
520
521
522
523
524
525
526
527
528
529
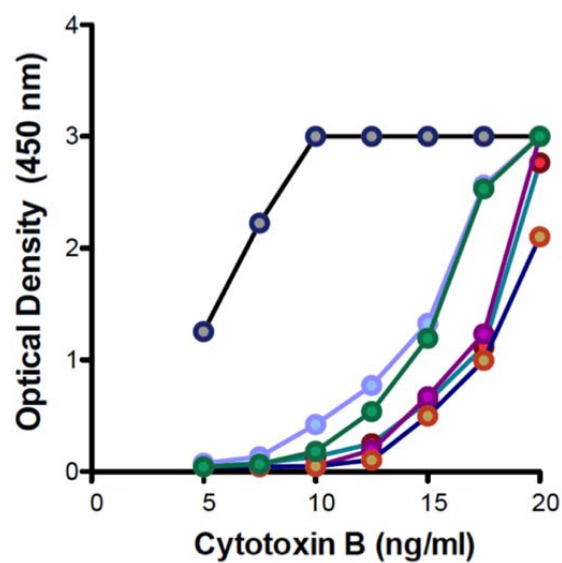
FIGURE 1. Untransformed EIA calibration curves. The mean optical density (*y*-axis) for each of six randomly selected cytotoxin B EIA calibration curves is plotted as a function of cytotoxin B concentration (*x*-axis). The data are expressed as means ± SEM.

530
531
532
533
534
535
536
537
538
539
540
541
542
543
544
545
546
547
548
549
550
551
552
553
554
555
556
557
558
559
560
561
562
563
564
565

A

B
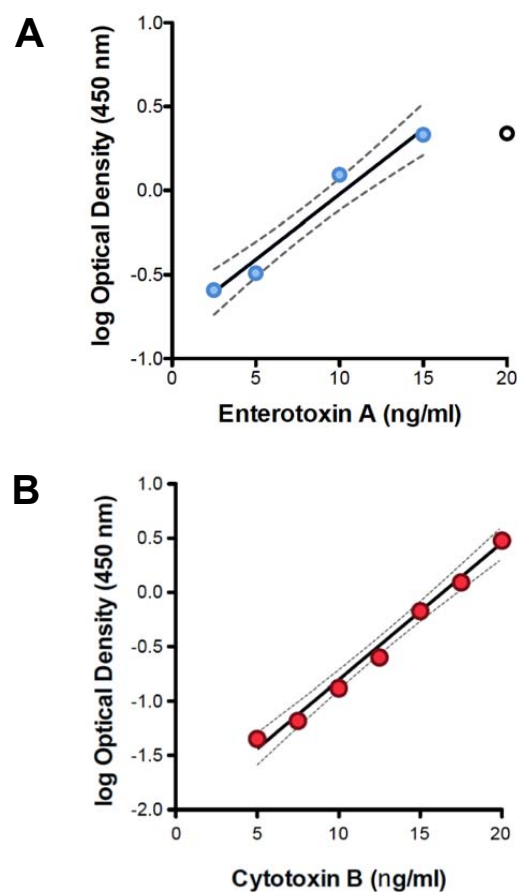
566 **FIGURE 2. Linear regression of representative logarithm-transformed qEIA**
567 **calibration data.** The logarithm (base 10) of the optical density of each reference
568 standard (*y-axis)* was determined by EIA and plotted against toxin concentration (*x*-axis).
569 Circles denote median calibration data from *n* repeated replicates. The solid line denotes
570 linear regression with 95% confidence limits, while dashed lines denote the boundaries of
571 the calculated 95% confidence interval. **Panel A,** linear regression of enterotoxin A data
572 ($n = 5$, $R^2 = 0.968$). **Panel B,** linear regression of cytotoxin B calibration data ($n = 4$, $R^2 =$
573 0.966).

574
575
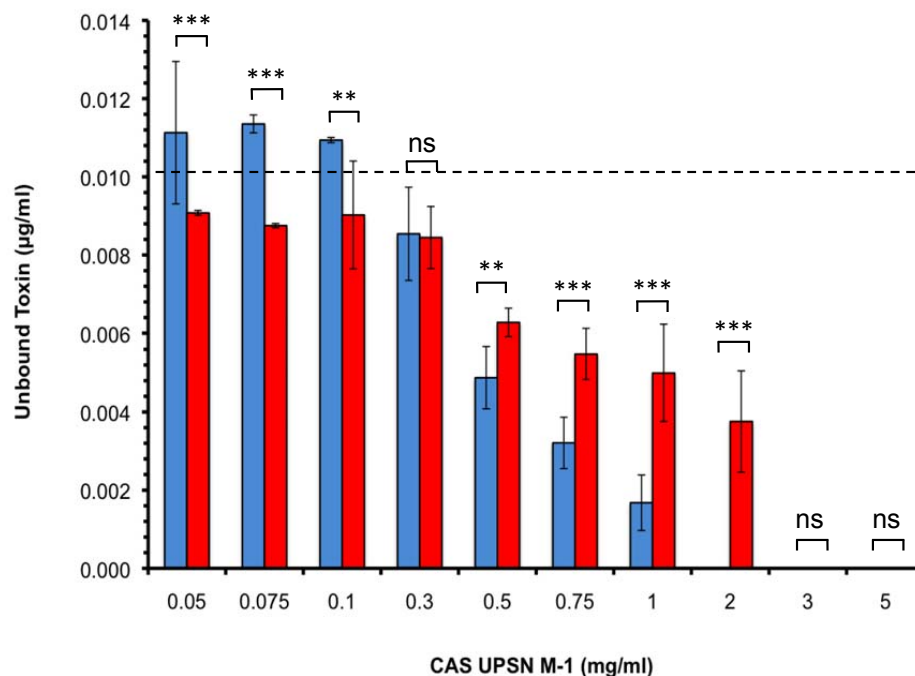
FIGURE 3. The selective and dose-dependent adsorption of *C. difficile* toxins by CAS UPSN M-1 *in vitro*. CAS UPSN M-1 was supplemented to a final concentration between 0.05 to 5 mg/ml (100-fold range) (*x*-axis), while toxin concentration was fixed to 10 μg/ml (dashed line). After a 10-min co-incubation, the mineral-toxin complexes were removed by centrifugation and the residual concentration of enterotoxin A (blue) and cytotoxin B (red) was determined by quantitative EIA (*y*-axis). The data are expressed as the means ± SD. The statistical significance of differences in toxin-specific binding-ability are reported for each concentration. Abbreviations: ns, statistically nonsignificant ($P > 0.05$); **, statistically significant ($P < 0.01$); ***, statistically significant ($P < 0.001$).

620
621
622
623
624
625
626
627
628
629
630
631
632
633
634
635
636
637
638
639
640
641
642
643
644

645

1 2 3 4 5

Myosin

BSA
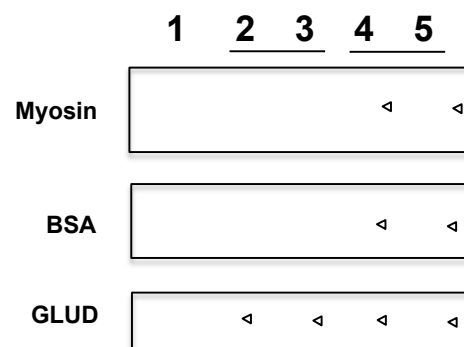
GLUD

646 **FIGURE 4. Non-therapeutic protein-binding assay.** SDS-PAGE gels illustrating
647 differential binding of myosin (top panel), bovine serum albumin (BSA) (middle panel),
648 and glutamate dehydrogenase (GLUD) (bottom panel). Lane 1, untreated reference
649 protein (negative control); Lanes 2-3, CAS UPSN M-1-treated protein samples
650 (duplicates); Lanes 4-5, eluate of protein-bound-CAS UPSN M-1 complexes (duplicates).
651 White carrots are used to mark lanes that are devoid of a protein band.

652

653